LA-UR -84-3503

Los Alamos National Laboratory is operated by the University of California for the United States Department of Energy under contract W-7405-ENG-36

TITLE POST IRRADIATION EXAMINATION OF FORT ST. VRAIN CRACKED FUEL ELEMENT SN1-2415

AUTHOR(S) Deborah R. Bennett
Keith E. Dowler
Jay H. Cook
Robert D. Reiswig

SUBMITTED TO US Nuclear Regulatory Commission

Los Alamos Los Alamos National Laboratory
Los Alamos, New Mexico 87545

FORM NO 836 R4
ST NO 2629 5/81

Post Irradiation Examination of Fort St. Vrain Cracked Fuel Element SN 1-2415

NRC Fin No. A-7258

October, 1984

Los Alamos National Laboratory

Deborah R. Bennett, Q-13

Keith E. Dowler, MST-14

Jay H. Cook, MST-14

Robert D. Reiswig, MST-6

Responsible NRC Individual and Division
J. Miller/ORB3

Prepared for the
U.S. Nuclear Regulatory Commission
Washington, D. C. 20555

DISCLAIMER

ABSTRACT

This report reviews the post-irradiation examination performed by Los Alamos National Laboratory on three slabs from the Fort St. Vrain cracked fuel element SN 1-2415. The slab cracks were photographically documented, and radiological, fractographic and metallurgical examinations were performed. The results indicate that the element graphite microstructure shows no unexpected features, and that the cracks found in element SN 1-2415 are typical of cracks found in comparable artificial graphites.

FORWARD

This technical evaluation report is part of the technical assistance program, "Review of Selected Fort St. Vrain Issues", FIN No. A-7258, and is supplied to the U.S. Nuclear Regulatory Commission, Office of Nuclear Reactor Regulation, by Los Alamos National Laboratory.

Post Irradiation Examination of Fort St. Vrain Cracked Fuel Element SN 1-2415 Technical Evaluation Report

Los Alamos National Laboratory
NRC Fin No. A-7258
October, 1984

1.0 Summary

Two adjacent graphite fuel elements removed from a common column of the Fort St. Vrain HTGR (High Temperature Gas-cooled Reactor) during the Segment 2 reload were found cracked axially along the B-face of each element, and cracked radially two and three webs toward the center of each element. A post-irradiation examination (PIE) was performed at Los Alamos National Laboratory on three slabs from the element with the wider crack, fuel element SN 1-2415.

The purpose of the examination was to investigate the crack microstructure, and to apply the results to a parallel analytical investigation of the cracking. The slab cracks were photographically documented, and radiological, fractographic and metallographic examinations were performed. The results indicate that the fuel element graphite microstructure has no unexpected features, and that the cracks found in element SN 1-2415 are typical of cracks found in comparable artificial graphites. This report describes the examinations performed, and the resultant conclusions based on the PIE findings. The parallel analytical evaluation of the crack mechanism will incorporate the results and conclusions of the PIE evaluation, and will be available at a later date.

2.0 Background

2.1 Core Position and Fuel Element Geometry

The Fort St. Vrain core is composed of 37 regions, each region containing 7 columns of hexagonal reflector and fuel elements, arranged so that the center column, which houses the control rod pair for the region, is surrounded by the remaining six columns, Figure 1. Each column is a stack of six active fuel elements, bounded by upper and lower reflector elements.

Each fuel element, Figure 2, is a hexagonal right prism, standing about 30 inches tall, and measuring approximately 14 inches from flat to flat. Each face of the element has a letter designation, from A to F; face E on each of the six outer columns in a region is oriented to the region's center column. On the upper axial end of each element, a set of three dowels interlocks with a set of three dowel sockets on the bottom end of the next element. The dowel designation corresponds to the element face notation.

Each graphite element has 210 fuel holes and 108 coolant channels drilled parallel to one another in a triangular array with 0.74-inch-pitch spacing, resulting in a basic ratio of two fuel holes for each coolant channel. All coolant channels and fuel holes are numerically designated as in the Fort St. Vrain Final Safety Analysis Report (FSAR)[5] and shown in Figure 3. The coolant channels are 0.625 inches in diameter, and are axially aligned with the channels in each element. Each fuel hole, 0.500 inches in diameter, is drilled from the top surface of the element, to within about 0.3 inches of the bottom. Bonded rods containing coated-fuel particles, each about 1/2 inch long, are stacked within the hole, and the hole is capped with a graphite plug. The fuel rods contain a homogeneous mixture of fissile particles containing both uranium^{235} (93.15% enriched) and thorium, and fertile particles containing only thorium. The carbide fuel particles are coated with a four-layer TRISO coating, and bonded into fuel rods with a coal tar pitch binder[2].

2.2 The Graphite Material

The element material is H-327 graphite, a petroleum-based, artificial graphite that is extruded into logs. The anisotropic graphite has coal tar pitch acting as the binder for the coke filler particles. The material is a so-called "needle coke", because the coke filler particles are relatively long and thin, and highly ordered. During the extrusion process, the acicular coke filler particles are preferentially aligned with their long axes parallel to the longitudinal (extrusion) axis, producing the observed anisotropy in the graphite logs. The general porosity observed in the graphite microstructure is an artifact of the production process, formed during baking and graphitization, as the pitch binder is pyrolized--i.e. the binder shrinks as volatiles (hydrogen, oxygen, carbon, and sulfur in various forms) are driven off, and the pores grow in size.

2.3 Background of Element SN 1-2415

Following the irradiation and removal of Core Segment 2 from the Fort St. Vrain (FSV) core in September, 1981, 54 fuel and reflector elements were subjected to a nondestructive examination[1] at the FSV hot service facility in April, 1982. During that examination, two of the fuel elements from Region 8, Column 5, at adjacent Levels 6 and 7, were identified as being cracked. In both cases, the cracks were located in the center of the B-face and appeared to run the full length of the element (in Region 8, Column 5, the B face is oriented towards the core center). The crack extended radially to coolant channel 319, and projected on to some undetermined position under the B-face dowel. A review of the pre-irradiation inspection reports indicated that neither element had been cracked prior to insertion into the core, and there was no record of damage during handling. It was therefore assumed that the cracks had developed during irradiation.

In the spring of 1983, the two cracked elements and three other elements were sent to GA Technologies (GAT) for more detailed visual examination. The visual examinations[2,3] showed that the cracks were the only apparent damage to the elements, and a stacking demonstration revealed no abnormal interaction between the dowel and sockets of the two elements when stacked in their

in-core configuration. Dimensional measurements, calculated temperature and fluence levels, and gross gamma activity for the two elements are listed in Table 1 as reference, and as reproduced from Ref. 4.

TABLE 1

Cracked Fuel Element Characteristics[4]

Item	SN 1-2415	SN 1-0172
Element Type	Fuel	Fuel
Core Location	08.05.F.06	08.05.F.07
Top Crack Width, mm	0.20-0.25	0.13-0.15
Bottom crack width, mm	0.28-0.30	0.05-0.08
Temperature, deg C (Time/volume avg)	650	700
Fluence, $x10^{25}$ n/m^2 $(E < 29\ fJ)_{HTGR}$	1.55	1.28

Because the presence of the B-dowel obscured the extent of the radial cracking, it was decided that the element with the more pronounced crack, SN 1-2415, would be subjected to destructive PIE. The PIE plan included Los Alamos National Laboratory, who would perform radiographic, metallographic and fractographic analyses on three one-inch slabs in verifying crack and graphite microstructure; GAT would use the remainder of the element in acquiring material property data[4]. The second element, SN 1-0172, would be stored, and analyzed only if required.

Initially, the extent of cracking in SN 1-2415 was confirmed by removing approximately a 1/4" slice from the top of the element, thereby effectively removing the cemented B-dowel from the element socket, without interfering with the fuel stacks. Photo 1 shows the top of SN 1-2415 after the removal of the first slice with the remainder of the B-dowel still in the socket. In this photo, the crack radially extends from the B face, across coolant channel 319, and disappears under the B-dowel. Photo 2, taken after the B-dowel section was removed, shows how the crack extended from coolant channel 319 to fuel channel 307, and on to coolant channel 295 under the B-dowel.

The element was further sectioned to remove the fuel stacks, and then three one-inch slabs were removed from the remainder of the element, according to Fig. 4, for shipment to Los Alamos.

3.0 Los Alamos Examinations

3.1 Visual Examinations

The three slabs cut from element SN 1-2415 were received at Los Alamos National Laboratory in August, 1983. The three slabs were labeled as Slab 1, 2 and 4, corresponding to the original location in the element. The slabs were in good condition, except that the striation patterns from the bandsaw cutting at GAT were apparent on both faces of each slab, and made verification of the crack location and extent more difficult.

A broad array of general and detailed photographs was taken of the three cracked regions, and provided a permanent record of the crack characterisitics on each slab prior to sectioning for other examinations. Photo 3. shows Slab 1, as seen in the Los Alamos hot cell facility, mounted on the rotatable jig used for positioning the slabs. Photographs 4 a, b and c show the crack definitely running from the B-face surface to coolant channel 319, over to fuel hole 307, and apparently traversing the graphite web over to coolant channel 295, for Slabs 1, 2 and 4, respectively. It was noted that the crack width seemed to narrow for each successive slab approaching the core midplane. A tabulation of the crack widths is available in Table 2.

TABLE 2
Crack Width Measurements

Slab	Approximate Crack Widths, inches x 10^{-3} B-face to 319	319 to 307	307 to 295
1	10-15	10-15	10-15
2	5-7	4-6	4-6
4	3-5	2-4	*

*Crack width not measurable by visual examination

Measurements were taken of selected fuel and coolant channels on both the B-face side and the opposite side of the element, to determine channel post-irradiation roundness. Generally very little ellipticity was found in the measured holes around the B-dowel region, or in channels across the slab, except for the holes with cracks. In all three slabs, the cracked holes were

ellipsoidal with the major axis parallel to the B-face, with a maximum 0.005 inches variation between the major and minor diameters. Measurement values are available in Appendix A.

3.2 Radiological Measurements

Radiological measurements were taken at the time of receipt, during which all three slabs indicated nominal radioactivity levels of 1.5 mr/hr, one meter from the slab faces. Edge surface measurements averaged 72 mr/hr, 50 mr/hr and 45 mr/hr, for slabs 1, 2, and 4, respectively, with a 40-90 mr/hr variation. Average face surface measurements were 445, 232, and 212 mr/hr, again for slabs 1, 2 and 4, respectively, with measurements ranging from 150-700 mrem/hr. Figures 5a, 5b and 5c indicate the relative radioactivity levels over each of the slabs, respectively. In general, the radioactivity levels of the three slabs were considered less than originally expected, allowing easier handling in the hot-cell environment.

Radiological information about the coolant and fuel channel surface areas was acquired with filter paper swipe samples, which were gamma analyzed using a Ge(Li) detector and a 4096 channel pulse height analyzer. A summary of the radioactive products found on the various surfaces is listed in Table 3. Fission products of U233 result in beta and gamma emitters such as Co144, Cs134, Cs137, Mn54 and Co60. The alpha emissions are from the thorium daughter products, but are at a negligible level. All radiological levels documented are well within anticipated ranges, and indicate that no unusual fission product migration to the coolant or fuel channel walls had occurred.

TABLE 3
Fission Product Activity Levels*

Location	Ce144	Cs134	Cs137	Mn54	Co60
Fuel Hole 307	0.1050	0.0155	0.0525	***	0.0372
Channel 319	0.0218	0.0026	0.0123	0.0061	0.1980
B-Face	0.1290	0.0248	0.0805	0.0267	0.8250
Top Surface	0.1460	0.0306	0.1010	0.0042	0.2550
Bottom Surface	0.0438	0.0112	0.0311	0.0084	0.3960

* Activity levels measured in microcuries

Autoradiographic techniques, where an x-ray type film is laid on the graphite surface and exposed by the resident radiation of the material, generally showed a tendency for relatively higher radiological levels around fuel holes 307 and 308. However, this qualitative technique also shows other areas relatively hotter, and the higher radiological levels are most likely artifacts of the slab cutting process, rather than an indicator of a radioactive anomaly.

3.3 Fractographic Analysis

Because Slab 4 was closest to the core midplane, it experienced higher power and fluence levels, relative to the other two slabs. For this reason, it was chosen for initial fractographic examination. The cutting plan in Figure 6 was used to expose one side of the crack fracture surface for each of the affected webs. Photos 5(a) and 5(b) (4x original magnification, but photographically reduced 22%) show the fracture surface in the webs between the B-face and coolant channel 319 and between coolant channel 319 and fuel hole 307, respectively. In both cases, the fracture surface is considered typical of tensile cracking. It was verified at this time that indeed no crack existed in the web between fuel hole 307 and coolant channel 295.

The SEM (Scanning Electron Microscope) photomicrograph in Photo 7 (original magnification as noted, but photographically reduced 4%) was taken on a sample of the fracture surface between the B-face and coolant channel 319, Slab 4, and shows how the graphite microstructure is a composite of dense, ordered coke filler particles, and unordered binder with porosity. With increasing magnification (50x, 100x, 200x), the greater long-range order of the coke filler particle relative to the surrounding material becomes more distinct--and it is that long-range order that allows basal-plane cleavage to take place within the particle. Assuming the needle-like coke filler particles are basically aligned in a given direction, it is not difficult to imagine a stress field operating to fracture the material preferentially in that direction.

3.4 Metallographic Examinations

The metallographic analyses included examining the graphite microstructure for possible anomalies, looking for differences between longitudinal and transverse microstructures, and determining crack paths. The metallographic samples from locations indicated in Figure 6 were prepared for examination by pressure-potting techniques--i.e. an epoxy resin was forced, under pressure, into the surface-accessible pores in the sample. Once the epoxy had set, the samples were ground and polished for examination. Photo 6 (32x original magnification, but photographically reduced 50%) shows typical microstructures obtained as described. The light features that have "grain" resembling that of wood are the coke filler particles. The binder areas are usually slightly darker, but are best identified using polarized light. The dark gray spots are pores filled with the epoxy mounting resin (note appearance of mounting resin at edges of samples). The few black spots that are visible are pores that did not fill with resin, and are considered to be sample preparation artifacts.

The H-327 graphite, as an anisotropic material, has distinctly different material property characteristics in the longitudinal (extrusion) and transverse directions, although this is not readily apparent in Photos 6(a) and 6(b) (32x original magnification, but photographically reduced 50%). This set of samples was taken from the web between the B-face and coolant channel 319, Slab 4, but is also typical of the longitudinal and transverse microstructure observed at several other locations in the slab.

The final examination on Slab 4 verified that no crack actually existed between fuel hole 307 and coolant channel 295. In Photo 8(a) (original magnification as noted, but photographically reduced 51%), the presence of a crack can not be directly identified because of the saw striation marks. Again, in Photo 8(b), no cracking could be found on the axial projection of fuel hole 307 or coolant channel 295 (not shown). But the photomicrograph of the web, shown in Photo 8(c), displays a string of pores between 307 and 295. Such a string is a good candidate path for crack propagation.

Slabs 2 and 1 were also used in verifying the localized crack morphology. Photo 9(a) (32x original magnification, but photographically reduced 49%) is a photomicrograph of the crack between the B-face and coolant channel 319, and 9(b) shows the central part at higher magnification (128x). At the center of

9(b) the crack can be seen to follow a path of easy cleavage along the grain of a coke filler particle. Photo 10(a) illustrates another energetically-favorable crack path, in which the crack tends to propagate so as to link up pores. Interestingly, no crack was found in the web between fuel hole 307 and coolant channel 295 in Slab 2.

Slab 1 was the only one of the three slabs to have cracks in the first three webs from the B-face, as shown in the sequence of Photos 11 and 12. Again, the general crack microstructure in Slab 1 echoed the patterns already observed in Slabs 2 and 4. Cleavage along the grain of filler particles and crack propagation between aligned, or even semi-aligned pores, seems to be the preferred mode of crack propagation in all slabs examined. This is consistent with what would be expected from the standpoint of lowest energy of formation, and is the crack mode usually found in artificial graphites.

It should be mentioned that during the sectioning process, the web between fuel hole 306 and fuel hole 294, Slab 1, broke. This area is within three webs of the B-face, but it is unclear whether the break was the result of propagating an incomplete, pre-existent crack, or if the crack was completely the result of handling. In examining Slabs 2 and 4, no evidence was found of cracking between fuel hole 306 and fuel hole 294.

4.0 Conclusions

In general, the results of the post irradiation examination on fuel element SN 1-2415 indicate that the microstructure of the graphite element shows no unexpected features. The crack extended two webs deep in the Slabs 4 and 2 where the power density was higher, and extended three webs deep in Slab 1.

The results from the radiological examinations show that residual activity in the graphite is very low and well within anticipated ranges. More importantly, the measurements indicate that no unusual fission product migration had occurred through any crack from fuel hole 307.

The results of the fractographic analyses indicated that the cracks found are typical of cracks found in comparable artificial graphites[6]. The fact that the crack remained open by a finite amount at the surface of the slab, tapering to zero width at coolant channel 295 and fuel hole 307 indicates that a system of balanced residual stresses existed in the element after the time of fracture. However, a method to determine the time of crack initiation and propagation is not available.

The metallographic examinations documented the tendency of the crack to propagate between pores and along the easy cleavage direction (i.e. the basal cleavage plane of filler particles). In all cases, the crack tended to follow the path of least resistance, in other words, the path that was most energetically favorable between the aligned pores and along coke filler particle cleavage planes. Samples taken from all three slabs confirm this as the mode for cracking.

In conclusion, the destructive post-irradiation examination of three graphite slabs from fuel element SN 1-2415 showed that no excessive fission product migration had occurred through the cracks, that the overall graphite microstructure had no unexpected characteristics, and that the fracture surface is typical of thermally-induced cracking.

References

1. Saurwein, J.J., "Nondestructive Examination of 54 Fuel and Reflector Elements From Fort St. Vrain Core Segment 2", GA-A16829, GA Technologies, October, 1982.

2. "Nondestructive Examination of FSV Fuel Element 1-2415", GA-A906505, GA Technologies, May, 1982.

3. "Visual Examination Results of Segment 2 FSV Fuel Elements 1-2415, 1-0172, 2-2693, 1-0108 and 5-0801", GA-906577, GA Technologies, October, 1982.

4. "Test Procedure for the Destructive Examination of Fort St. Vrain Fuel Element 1-2415", GA-A906770, GA Technologies, Febraury, 1983.

5. Fort St. Vrain Nuclear Generating Station, "Updated Final Safety Analysis Report," Public Service Co. of Colorado.

6. Private communication with Robert D. Reiswig, MST-6, Los Alamos National Laboratory, 1984.

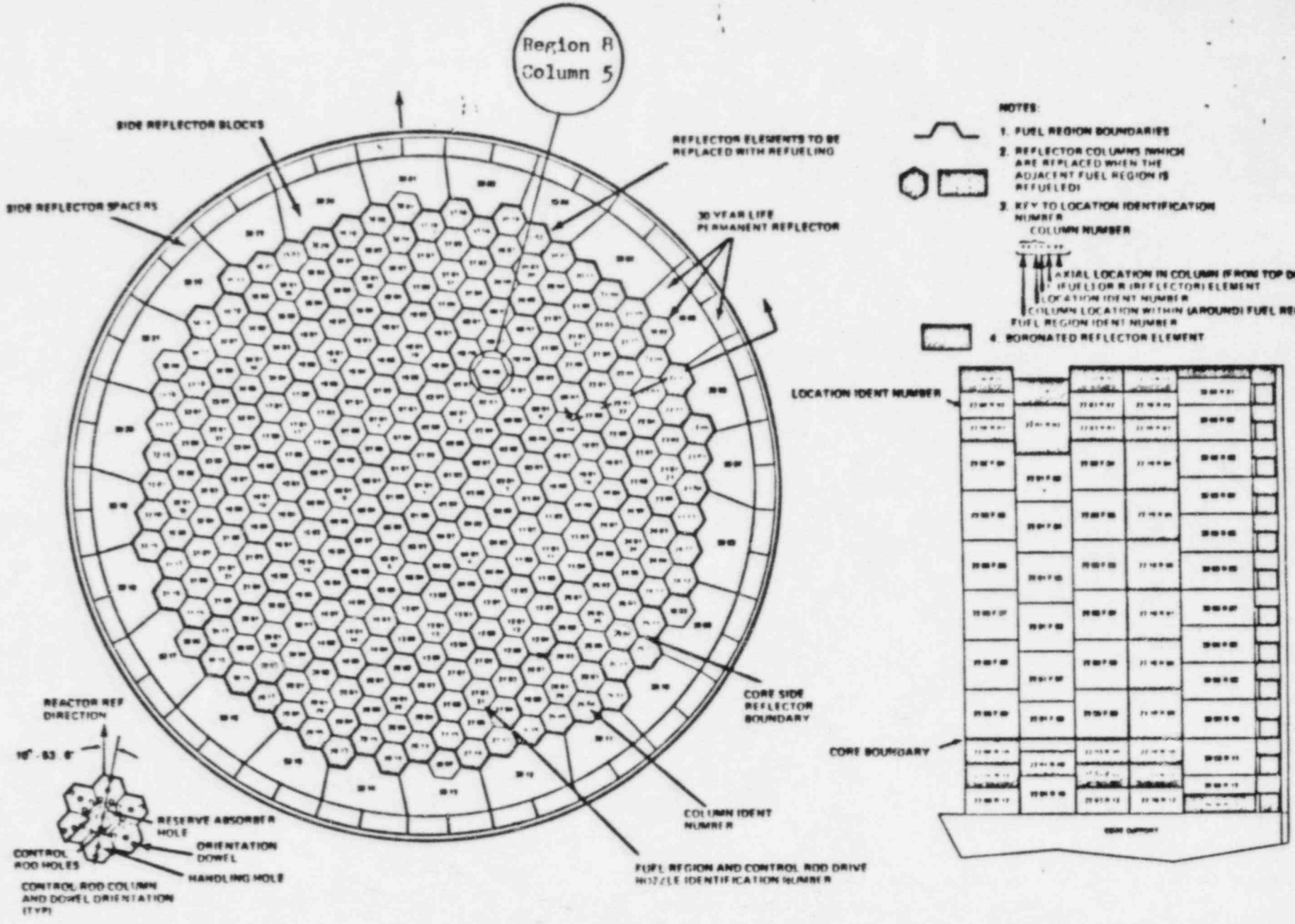

Figure 1. FSV Core Arrangement

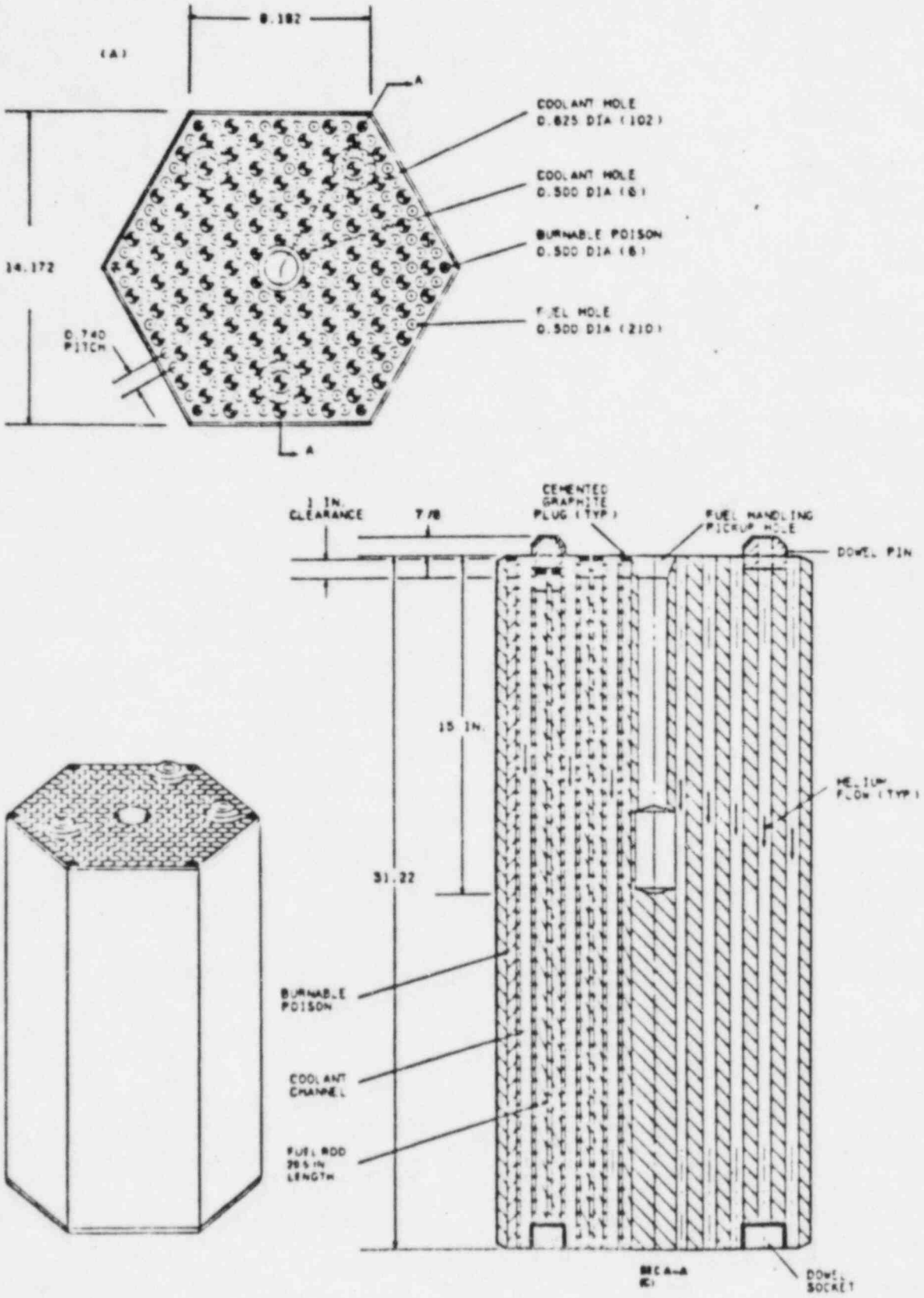

Figure 2. Fuel Element Geometry

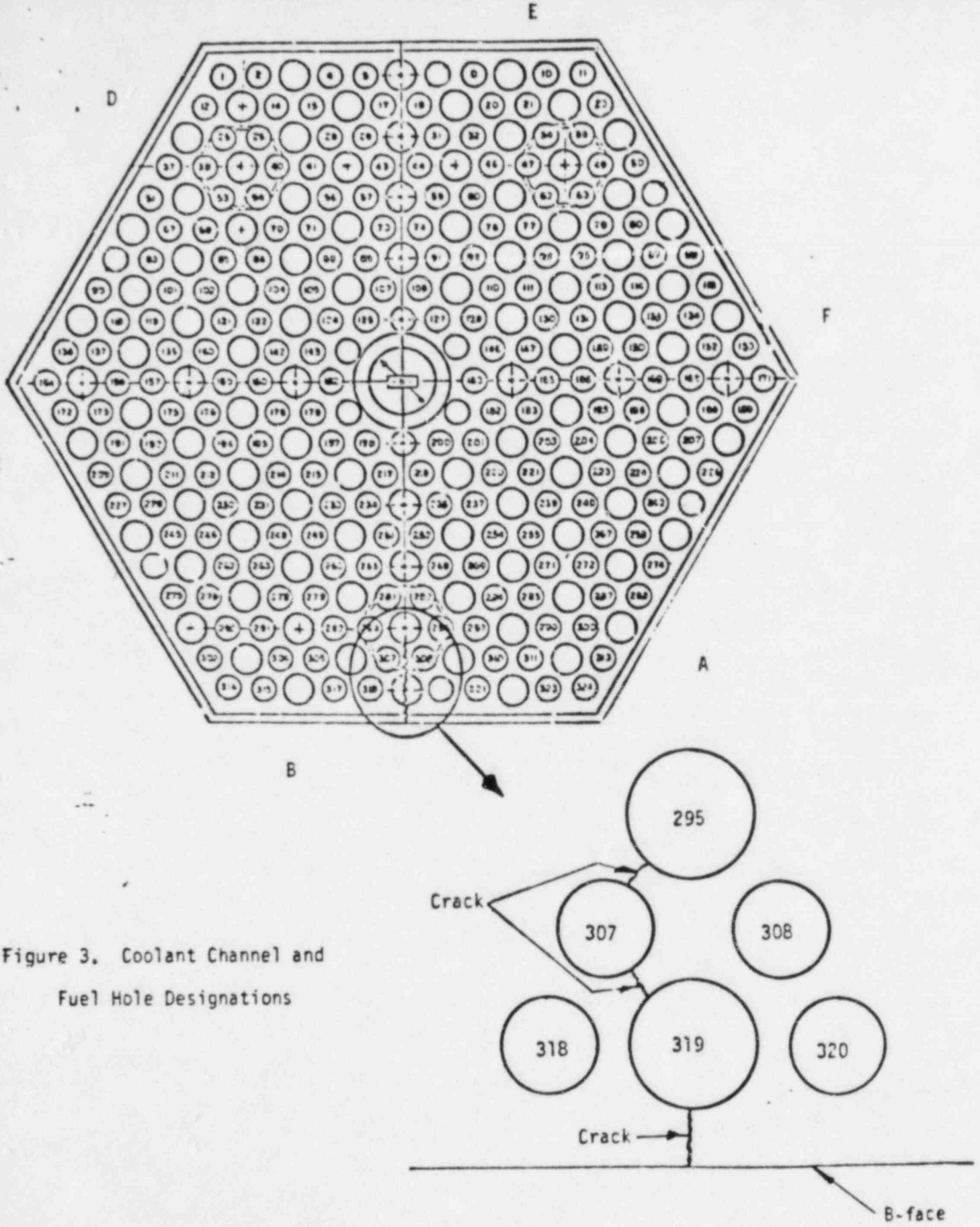

Figure 3. Coolant Channel and Fuel Hole Designations

Figure 4. Element SN 1-2415

Sectioning Plan

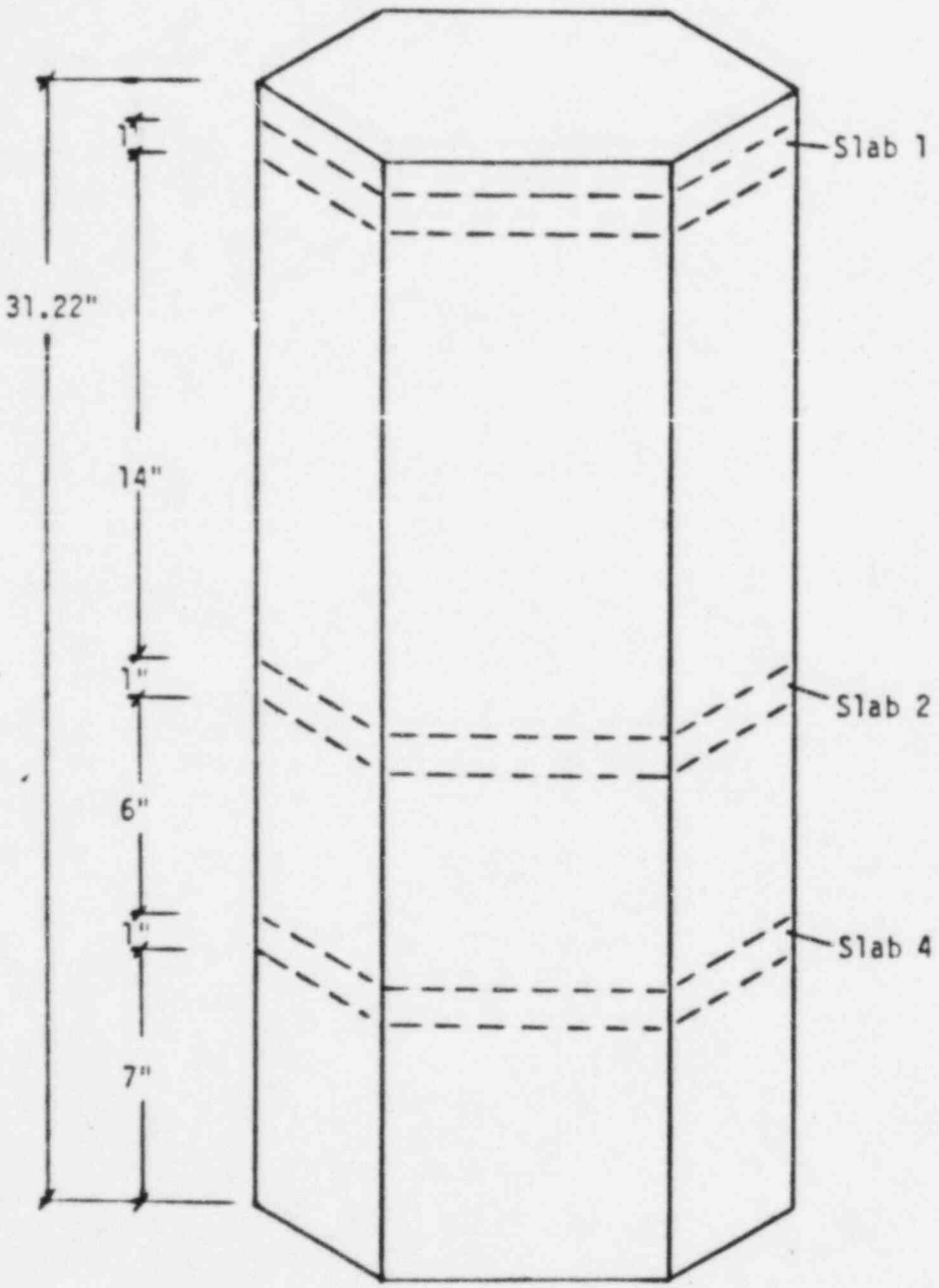

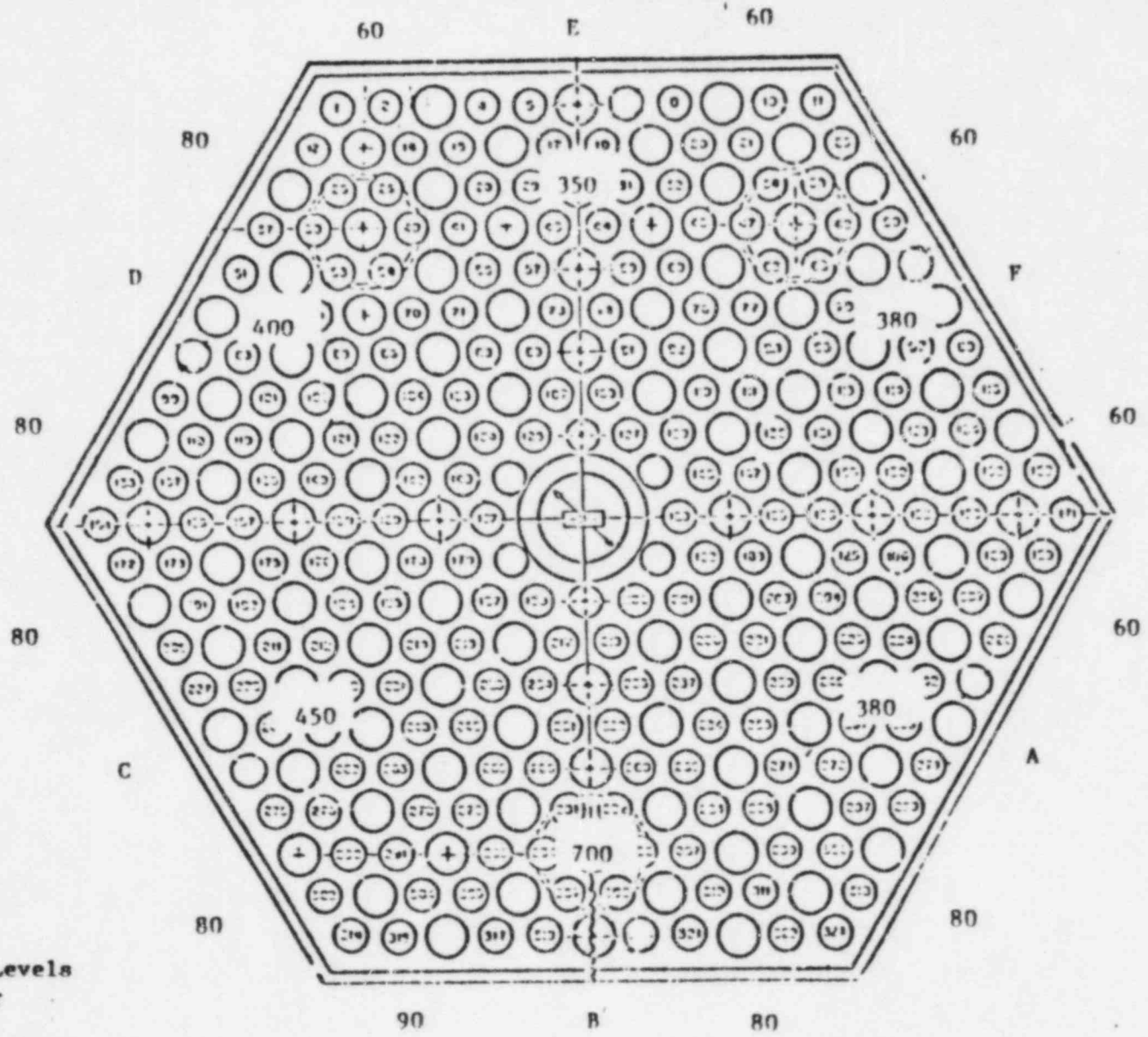

Fig. 5a Radiological Measurements

Slab 1

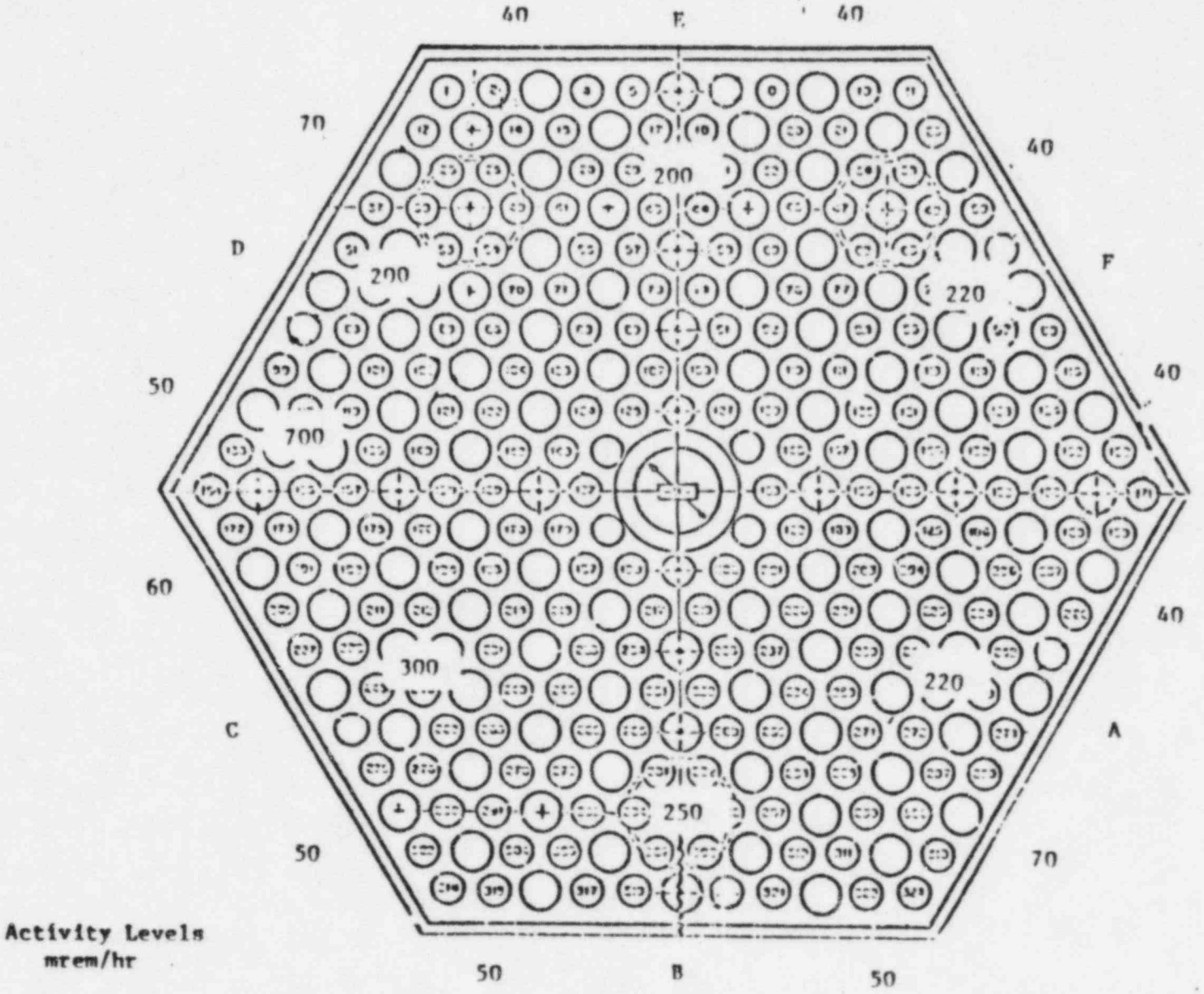

Fig. 5b Radiological Measurements

Slab 2

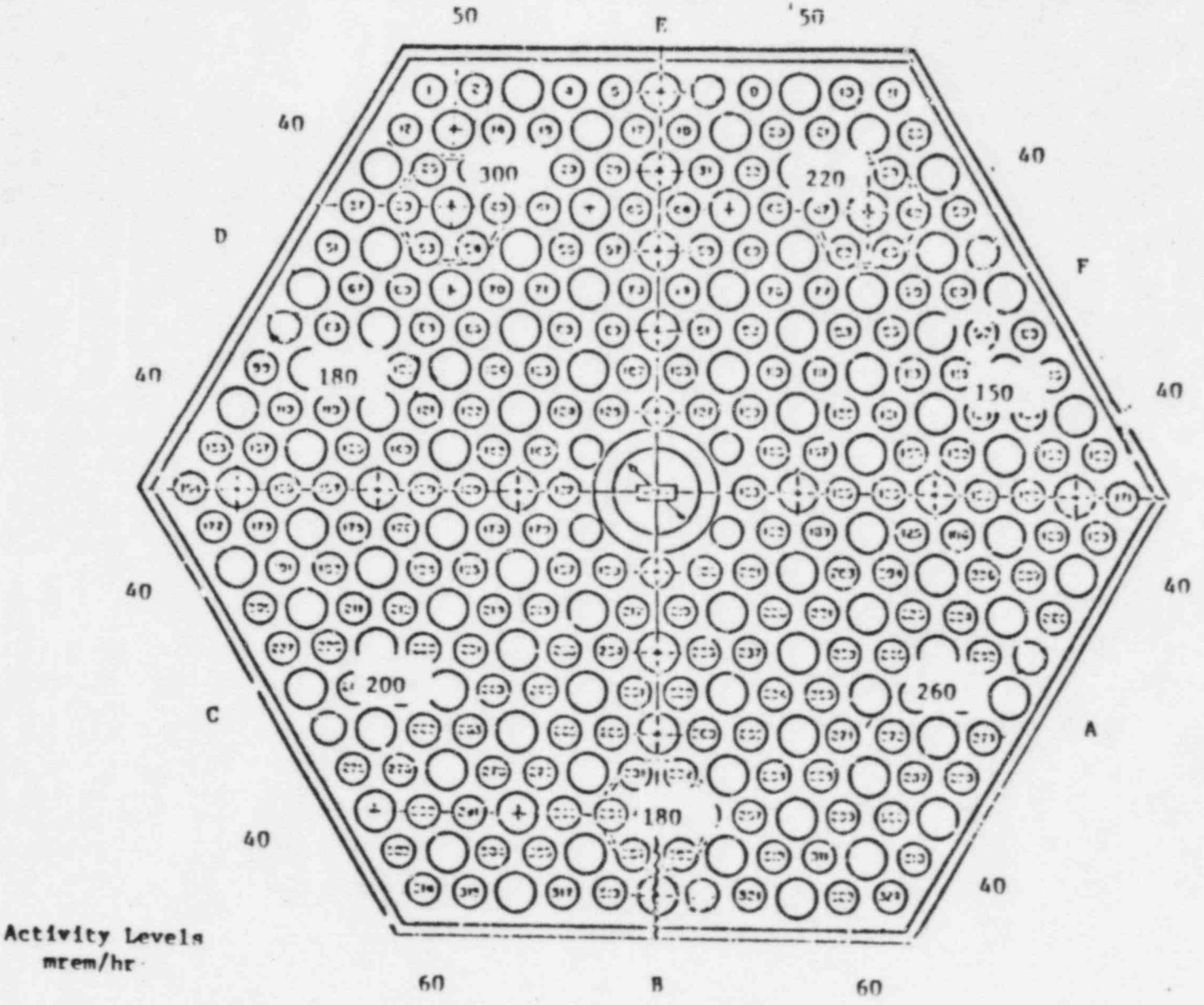

Fig. 5c Radiological Measurements

Slab 4

Figure 6. Fractographic and
metallographic Sectioning

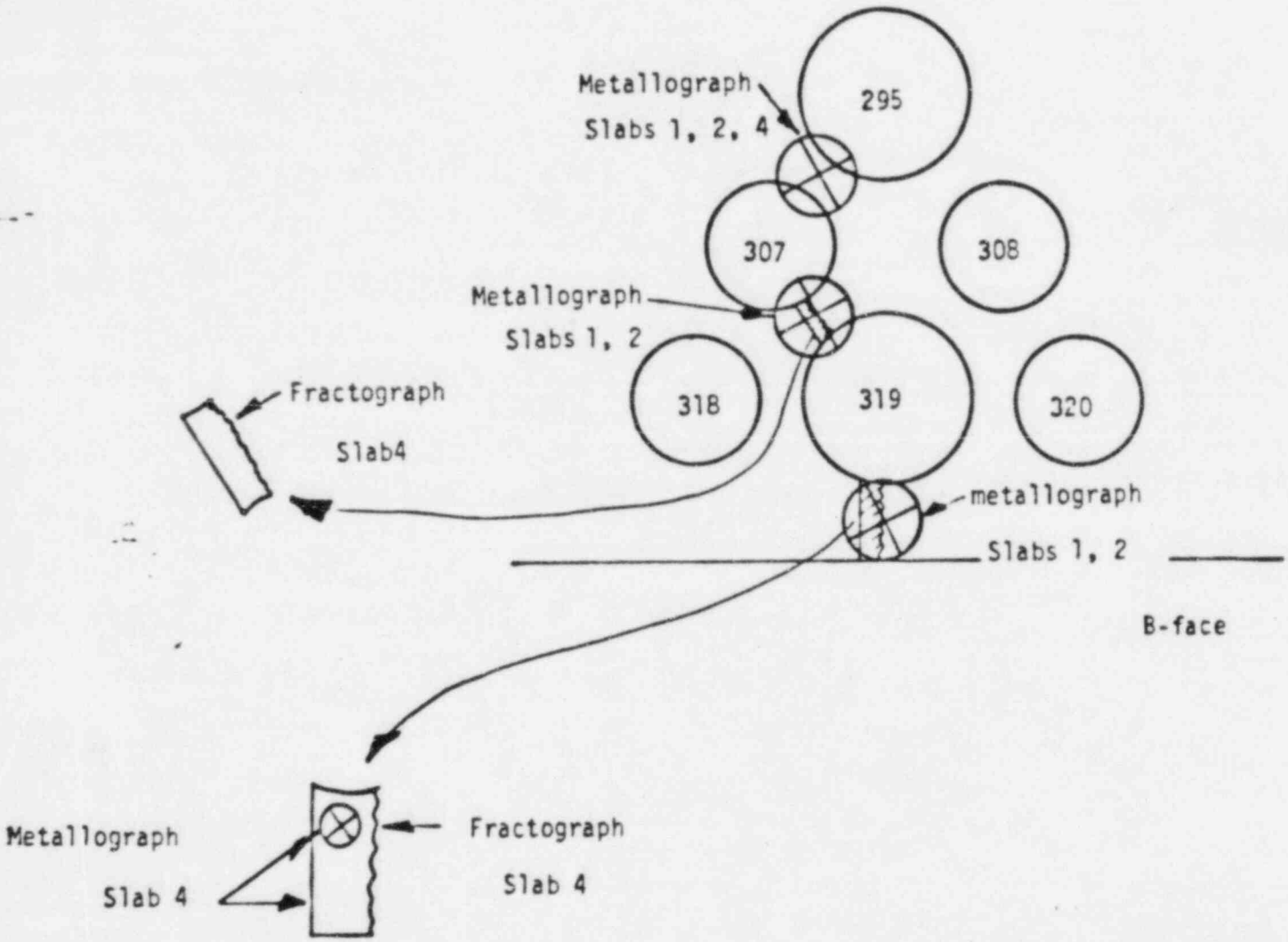

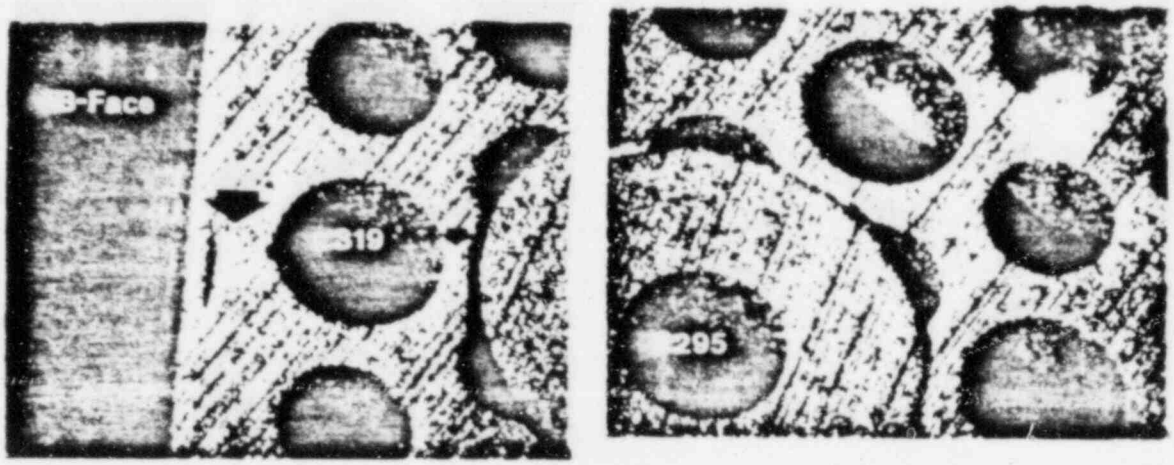

SN 1-2415 Element--Slice
removed showing B dowel

Photo 1

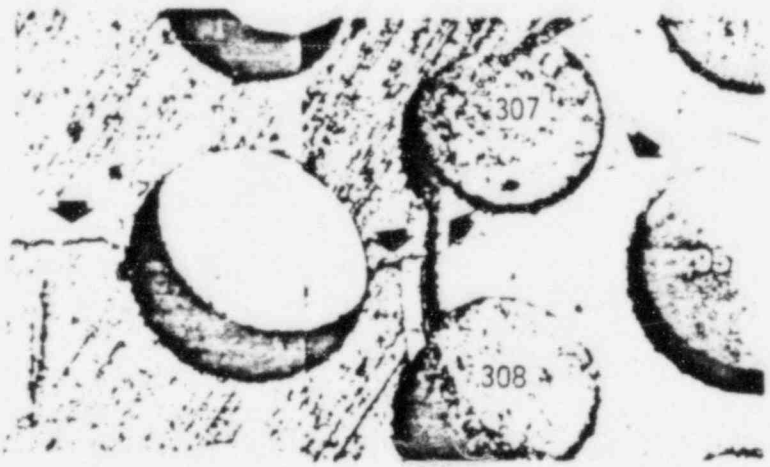

Top of GAT Slice, showing
crack in dowel socket

Photo 2

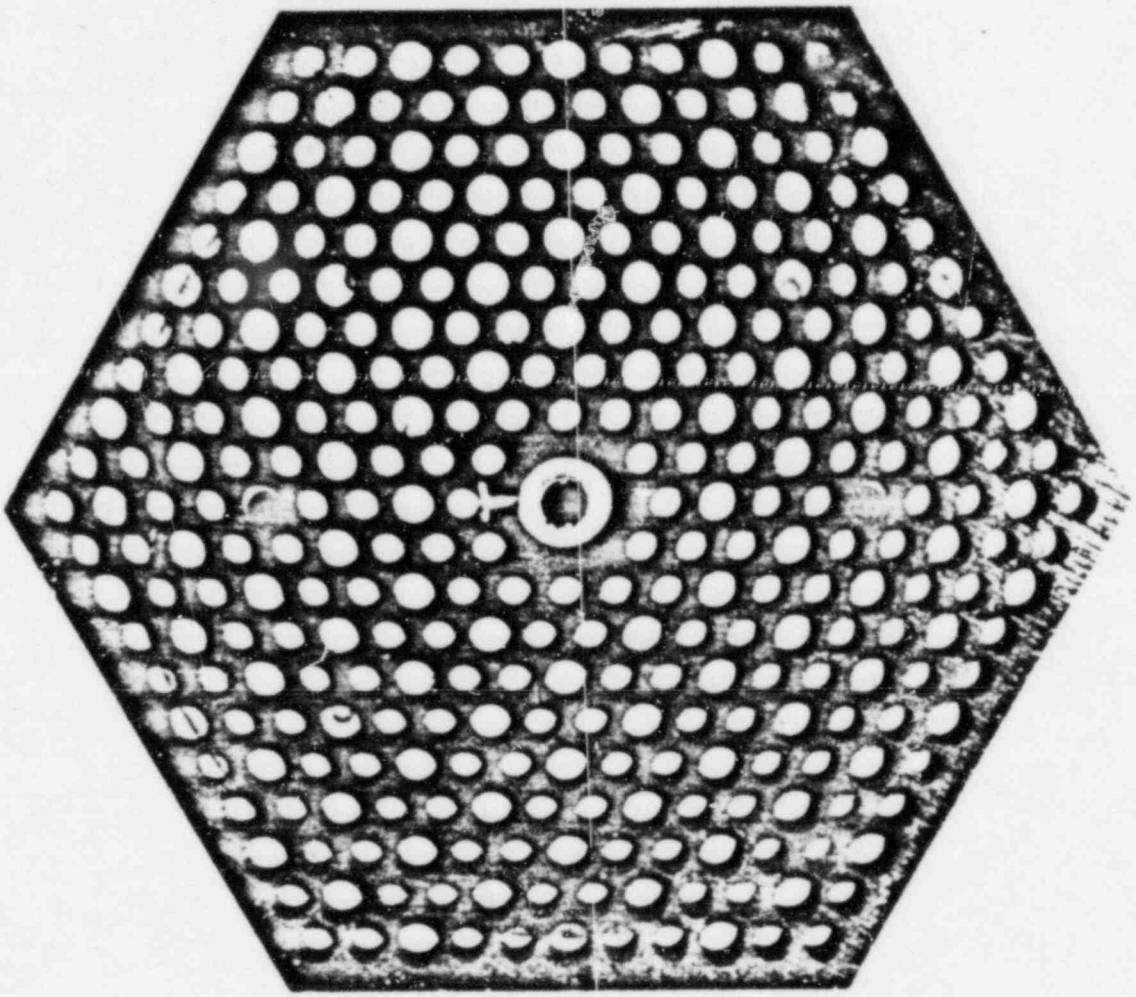

B-Face

Q13-5

FT ST URAIN
FUEL BLOCK S/N 1-2415
SECTION 1-TOP

Photo 3

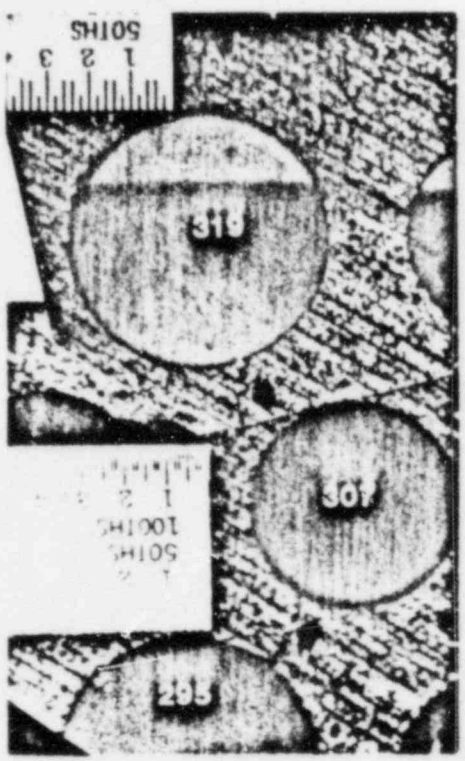

SECTION 1

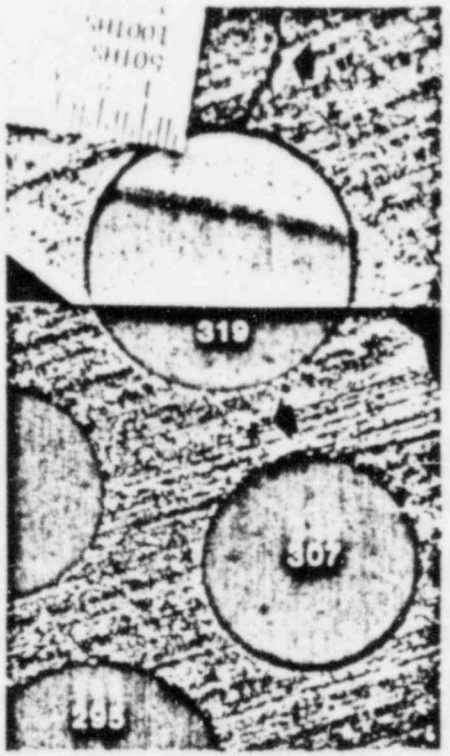

SECTION 2

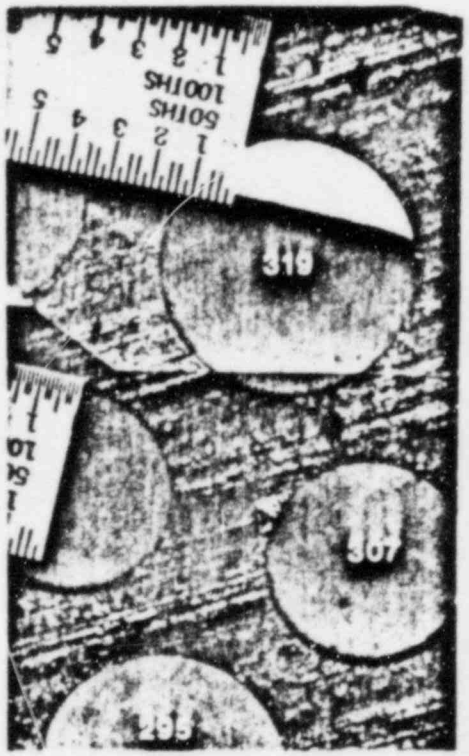

SECTION 4

Photo 4

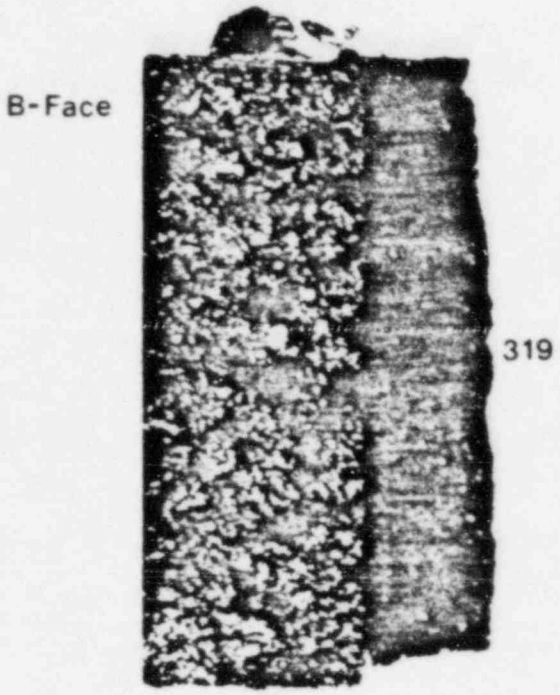

Photo 5(a)

Fracture surface between
B-Face and 319. Slab 4
4x

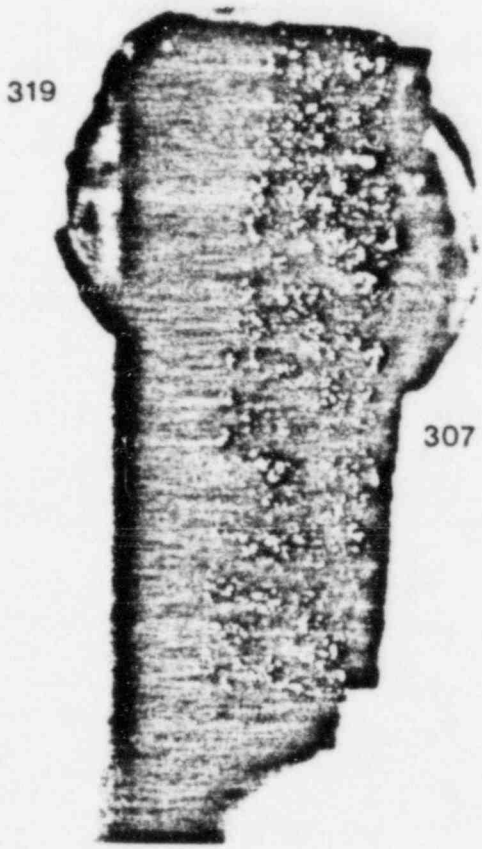

Photo 5(b)

Fracture surface between
319 and 307. Slab 4
4x

Photo 6(a)

Photomicrograph of Longitudinal cross section between B-Face and 319, Slab 4

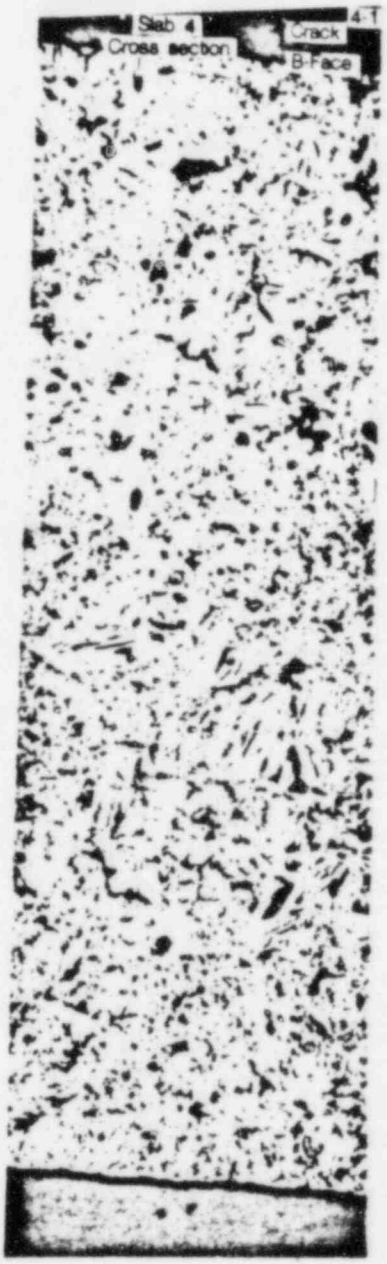

Photo 6(b)

Photomicrograph of Transverse cross section between B-Face and 319, Slab 4

SEM (Scanning Electron Microscope) Photomicrograph showing cleavage, Slab 4

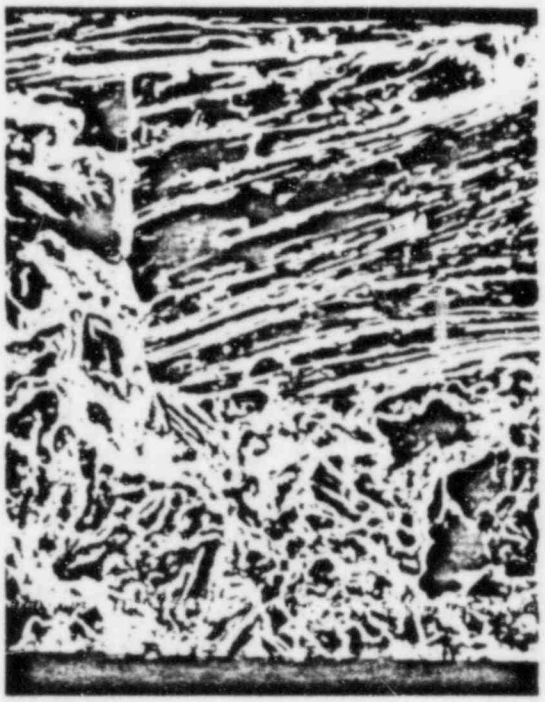

Photo 7(b) 100x

Cleavage in dense area

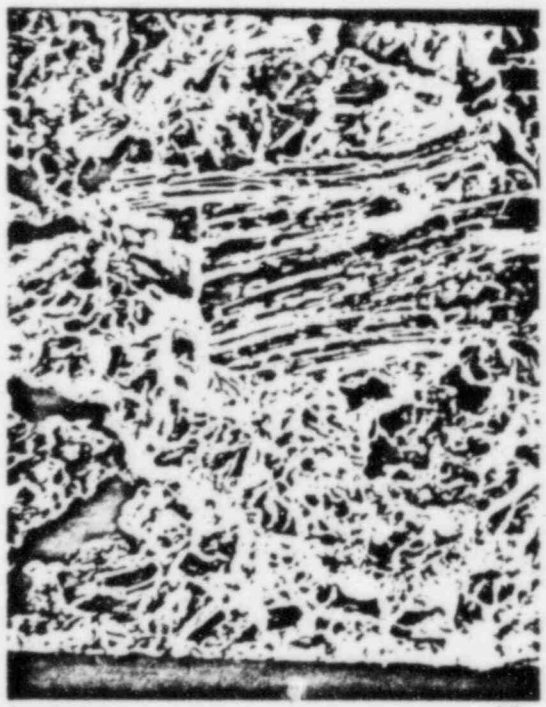

Photo 7(a) 50x

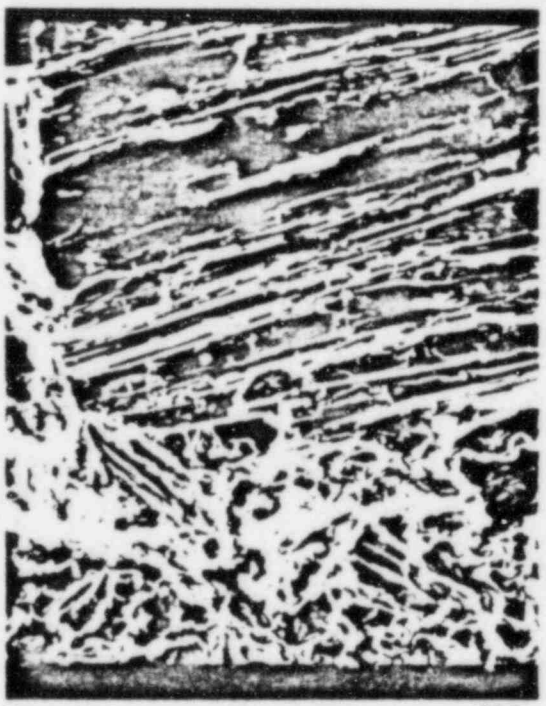

Photo 7(c) 200x

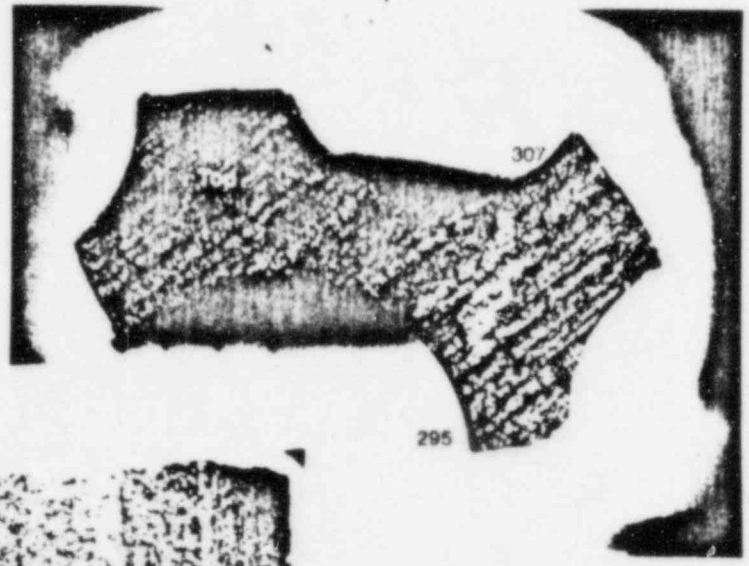

Photo 8(a)

Web between 295 and 307 has no indication of cracking when magnified 8x

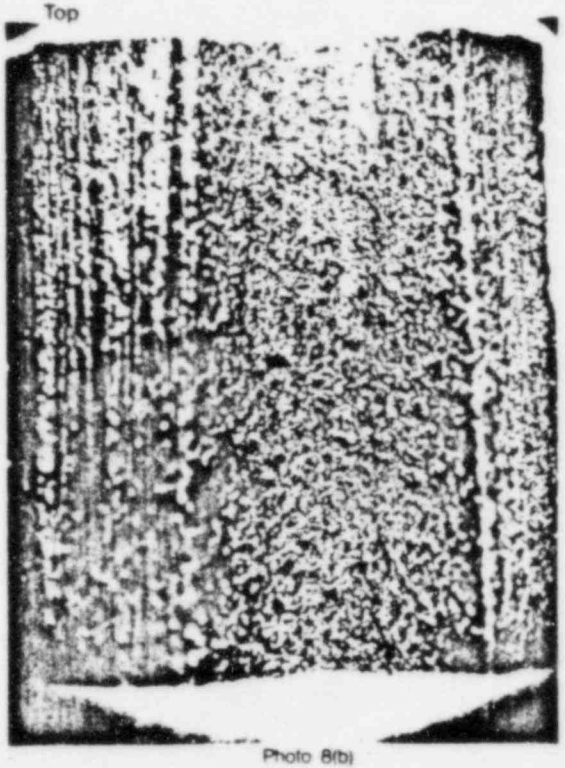

Photo 8(b)

Looking at side edge of 307, towards 295, shows no sign of axial cracking at 8x

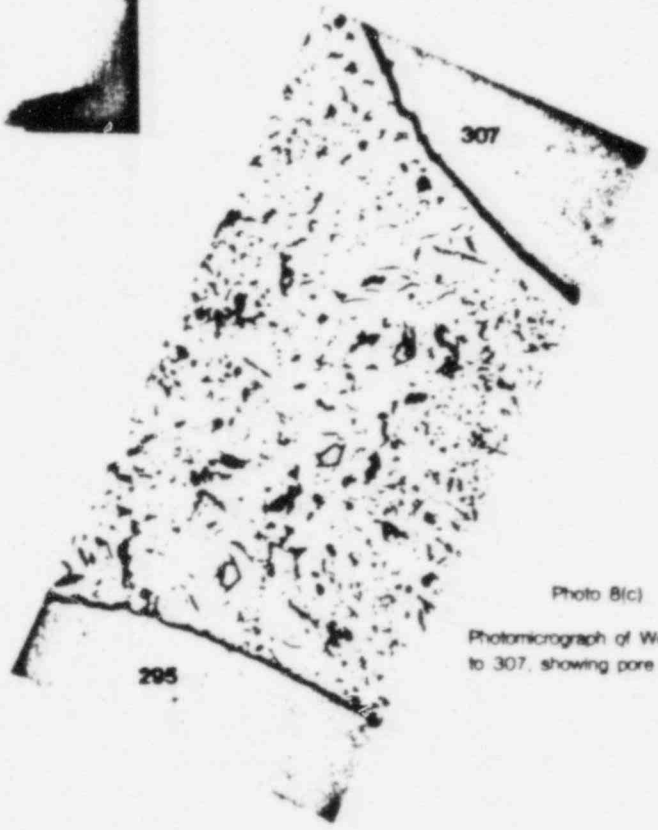

Photo 8(c)

Photomicrograph of Web 295 to 307, showing pore alignment

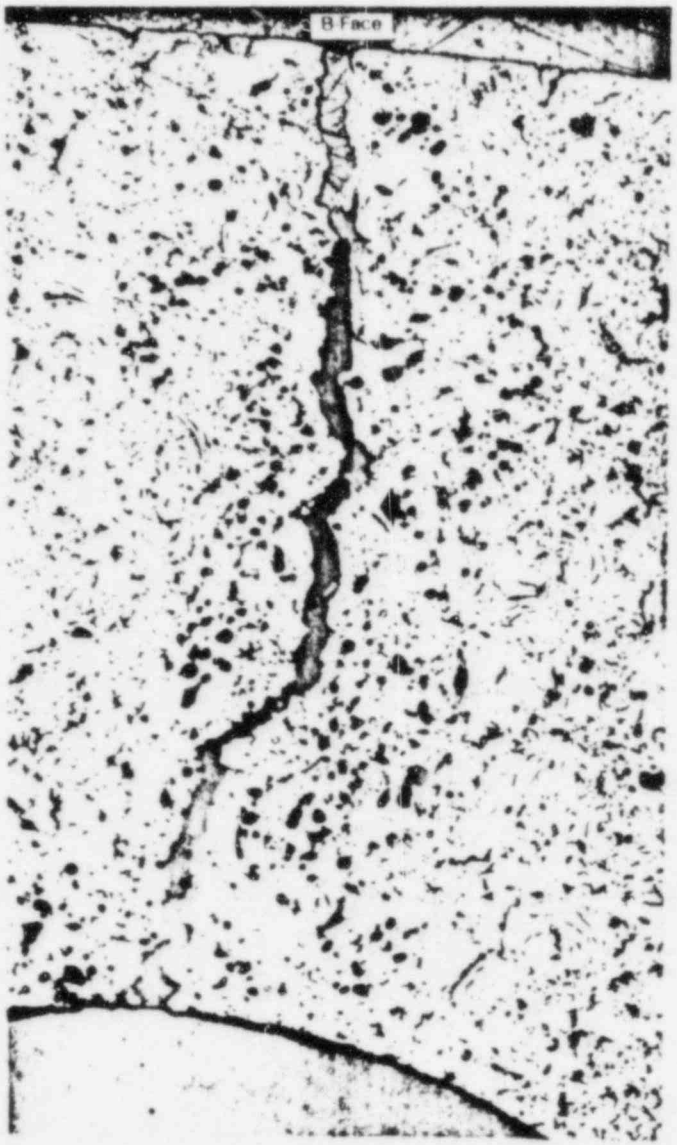

Photo 9(a)

Photomicrograph of crack between B-Face and 319 Slab 2

Photo 9(b)

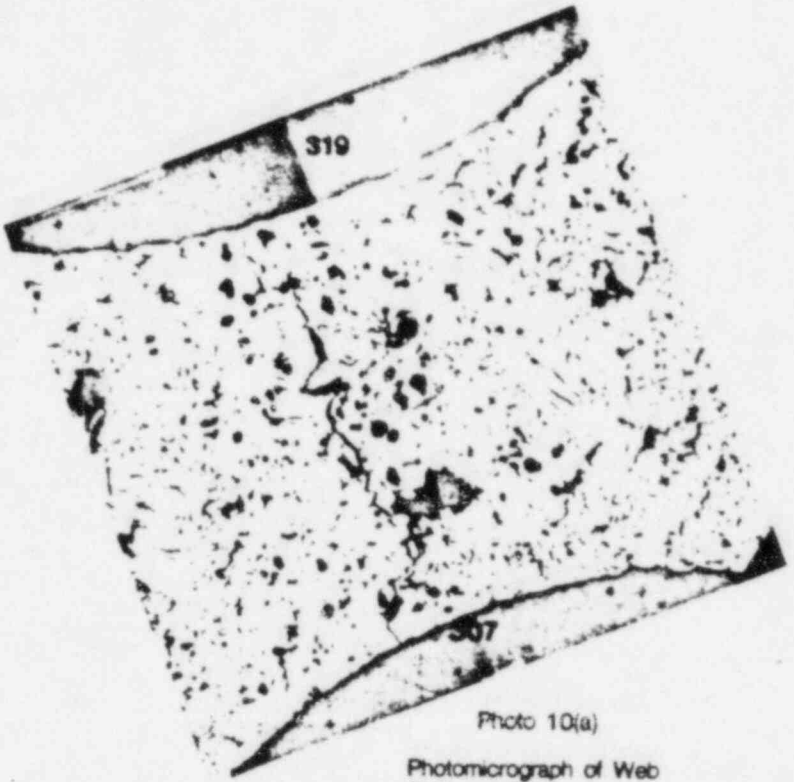

Photo 10(a)

Photomicrograph of Web 319 and 307, Slab 2

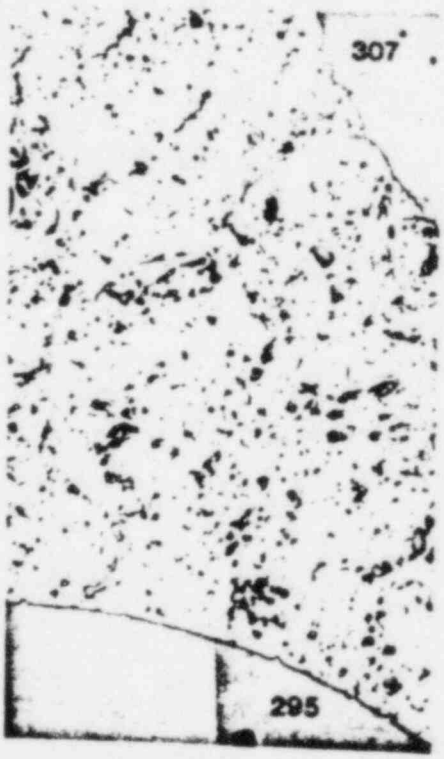

Photo 10(b)

Photomicrograph of Uncracked Web between 307 and 295, Slab 2

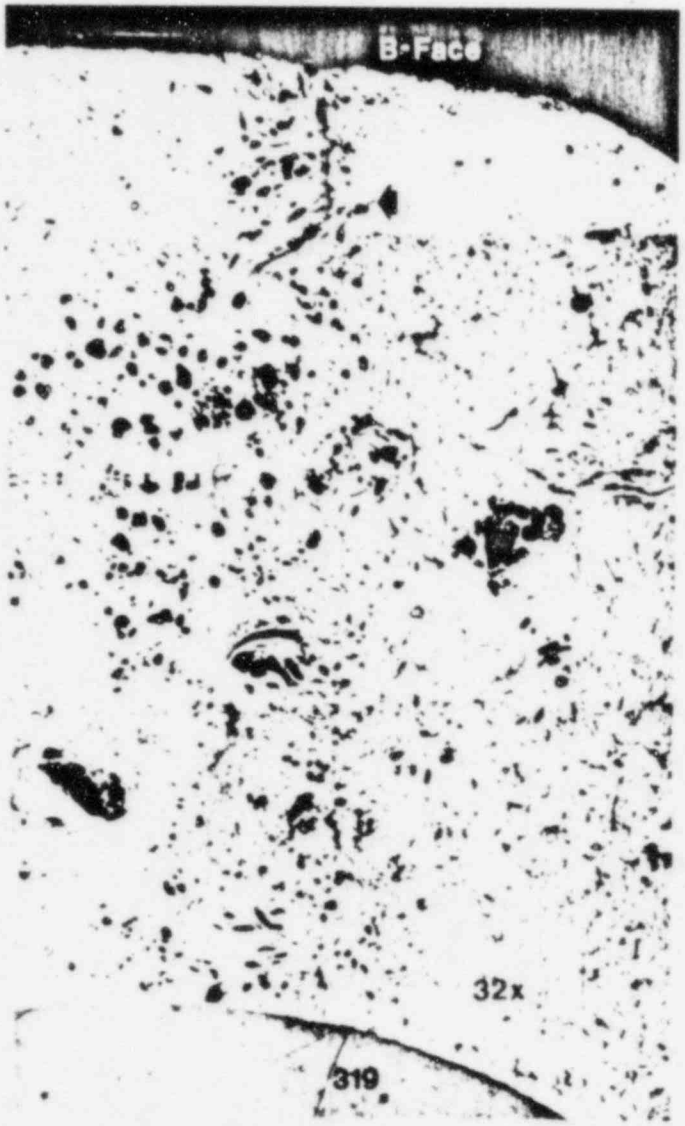

Photo 11(a)

Photomicrograph of Web
between B-Face and 319
Slab 1, 32x

Photo 11(b)

Photomicrograph of Crack Segment
1 between B-Face and 319
Slab 1, 128x

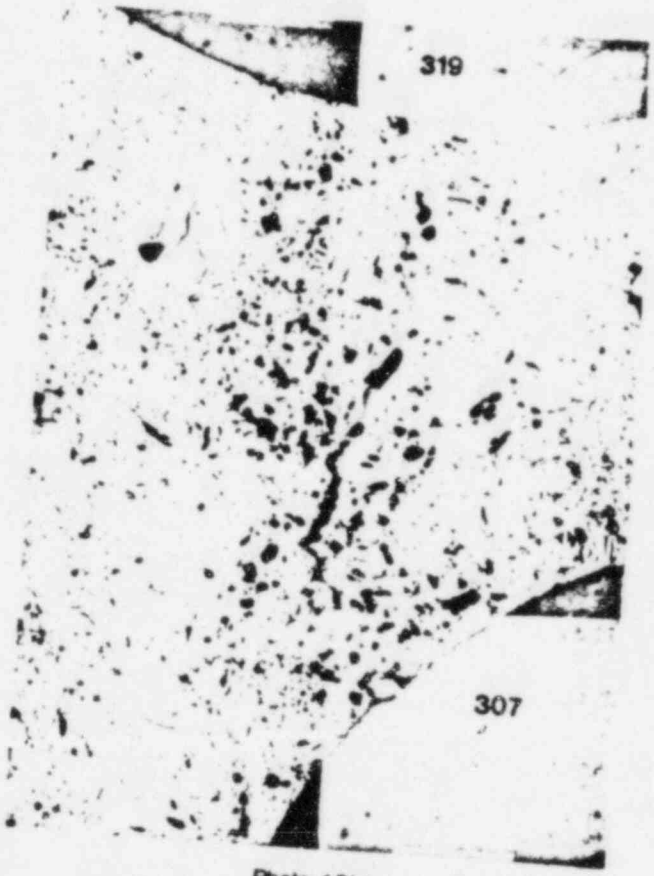

Photo 12(a)

Photomicrograph of Web between 319 and 307, Slab 1

Photo 12(b)

Photomicrograph of Web between 307 and 295, Slab 1

Appendix A

"B" SURFACE

SECTION #1 TOP	A	B	C	D
HOLE # 316	.620	.621	.621	.621
HOLE # 317	.497	.497s	.497	.497s
HOLE # 318	.496	.497s	.497s	.497
HOLE # 319	.626	.624	.621s	.625
HOLE # 320	.497	.497s	.497s	.497s
HOLE # 321	.497	.497	.497s	.497s
HOLE #322	.621	.621	.621	.621
HOLE # 295	.623s	.623	.621s	.622
HOLE # 307	.497s	.497s	.497s	.497
HOLE # 308	.497	.497s	.497s	.497
HOLE # 6	.622	.622	.622	.622
HOLE # 17	.498	.498	.498	.498
HOLE # 18	.498	.498	.498	.498
HOLE # 30	.622	.622	.622	.622

Rich Thomas

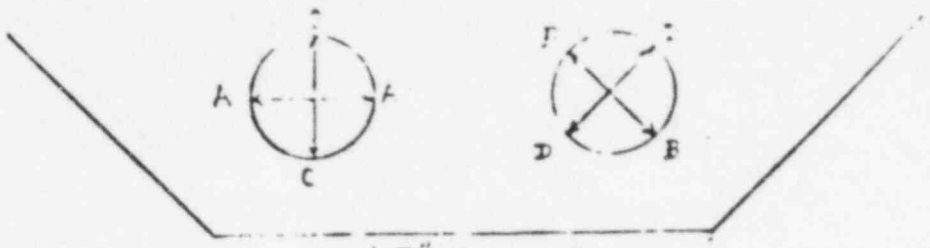

Section #2 Top	A	B	C	D
HOLE # 316	.621	.621	.621	.621
HOLE # 317	.497s	.497s	.497s	.49?
HOLE # 318	.497s	.497s	.497s	.498
HOLE # 319	.625	.624	.622	.624
HOLE # 320	.497s	.498	.497s	.497
HOLE # 321	.497s	.498	.497s	.497
HOLE #322	.621	.621	.621	.621
HOLE # 295	.621	.622	.622	.621s
HOLE # 307	.498s	.498	.498	.498
HOLE # 308	.498	.497s	.498	.498
HOLE # 6	.622s	.622s	.622s	.622s
HOLE # 17	.498	.498s	.498	.498s
HOLE # 18	.498s	.498s	.498s	.498s
HOLE # 30	.622s	.622s	.622s	.622s

R.A.D. Dennison

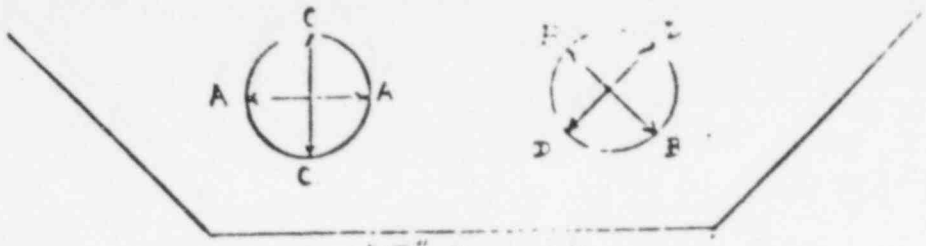

"B" Surface

Section #4 Top	A	B	C	D
HOLE # 316	.621	.621	.621	.621
HOLE # 317	.497s	.498	.497s	.498
HOLE # 318	.497s	.497s	.497s	.498
HOLE # 319	.625s	.624	.622s	.624
HOLE # 320	.498	.498s	.497s	.497
HOLE # 321	.497s	.498s	.497s	.497
HOLE #322	.621s	.621s	.621	.621
HOLE # 295	.621c	.621c	.622	.621s
HOLE # 307	.498c	.498s	.498	.498
HOLE # 309	.497s	.497s	.497s	.498
HOLE # 6	.622s	.623	.622s	.622s
HOLE # 17	.498s	.498s	.498s	.498s
HOLE # 18	.499	.499	.499	.499
HOLE # 30	.622s	.623	.622s	.622s

EHS Thomas